

Propagation of HF radio waves on short high latitude paths

Olga A. Maltseva, Tatyana V. Nikitenko

Institute for Physics, Southern Federal University, 344090, Rostov-on-Don, Russia, mal@ip.rsu.ru

Abstract

The joint use of experimental data and modeling methods on the high-latitude Gorkovskaya-Lovozero path with a length of $D \sim 900$ km made it possible to test several methods for determining the maximum useable frequency using the IRI model: 1) ray tracing method, 2) Smith method. In the latter case, the propagation coefficient MD(IRI) was used for the path length D and various options for determining the critical frequency f_oF_2 in the middle of the path. The results relate to the conditions of minimum solar activity (May 2017-January 2018). It was found that the second simple method using the original IRI model yielded a result comparable to the result of the ray tracing method with model adjustment to the full set of vertical sounding data. The method of using the total electron content, which proved to be good under conditions of high solar activity, led to significantly underestimated results.

1 Introduction

Currently, interest in the high-latitude ionosphere, responsible for the propagation of HF radio waves, has significantly increased. Despite the widespread (and even predominant) use of satellite communications, HF communications has not lost its significance, especially in high-latitude areas. This is directly related to the method of oblique sounding. However, the situation here is not ideal: additional efforts are needed for experimental studies and to increase the accuracy of determining parameters such as f_oF_2 , h_mF_2 , MUF, M3000, and others, using empirical models of the ionosphere. This is especially true for conditions of low solar activity, when scientists were faced with increased inaccuracy of models (e.g. [1]).

The aim of the work is to obtain experimental data for these parameters and compare them with the most common IRI model [2]. In this paper, we use the data of the daily variations plots of the ionosphere parameters of the two stations Gorkovskaya (60.27° N, 29.38° E), Lovozero (67.97° N, 35.02° E) such as f_oF_2 , h_mF_2 and the maximum useable frequency (MUF) on the Gorkovskaya-Lovozero path ~ 900 km length provided by AARI on the website (<http://geophys.aari.ru/>), for the period with the most data from May 2017 to January 2018. The IRI2016 online version on the website (http://omniweb.gsfc.nasa.gov/vitmo/iri2016_vitmo.html) was used to avoid inaccuracies associated with the introduction of new solar indices [3].

2 MUF Comparison

Three options are considered, for which are compared: A) the medians of the experimental MUF3000F2 values for two selected stations for several months with each other and with the IRI model, B) the MUF900 values calculated by the method of ray tracing using the original IRI model and its adaptation to the parameters of the current diagnostics, with experimental MUF900 for the Gorkovskaya (GRK) - Lovozero (LOZ) path, C) MUF900 values calculated using the coefficient MD and f_oF_2 in the center of the path.

2.1 Comparison of Medians of MUF

The medians of the MUFs of the two stations are compared to determine the climatological features of the behavior of this parameter. Figure 1 shows the behavior of the MUF3000F2 for the months of the solstice, equinox of 2017 and January 2018. For each station, experimental and model values are given.

It should be noted that the Gorkovskaya station lies close to mid-latitudes, and the Lovozero station lies in the auroral zone. This leads to differences in behavior. Firstly, it can be seen that a median can be absent. This indicates that for a whole month at this hour there was not a single measurement.

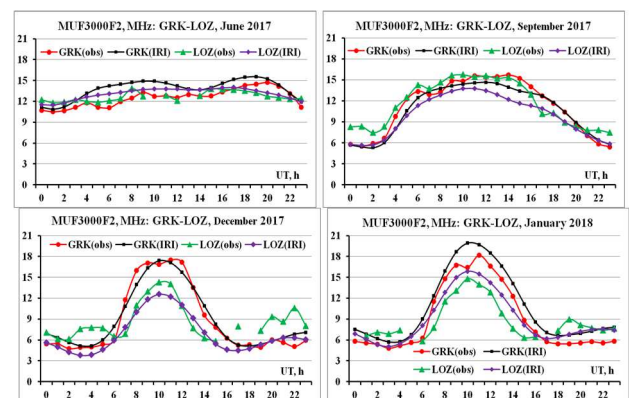


Figure 1. Peculiarities of the behavior of model IRI values and medians of the MUF3000F2 of two stations in 2017 and in January 2018

Secondly, a feature of the auroral zone is the intensification of night ionization, especially in winter.

Third, the greatest differences in the values of the two stations also apply to winter time, with daytime winter values exceeding summer ones. The differences between the model and experimental values are not so great. Quantitative characteristics are given in Tables 1-2 in the form of standard deviations σ of the model parameters M3000F2 and MUF3000F2 from the experimental values presented for both median and instant (ins) values characterizing day-to-day variations. Each table is divided on two parts on five columns separately for parameters M3000 and MUF3000 for reduction of the paper space. Table 1 represents the station Gorkovskaya, Table 2 – Lovozero.

Table 1. The standard deviations of the model parameters M3000F2 and MUF3000F2 from the experimental values for the Gorkovskaya station

	M3000			
GRK			%	%
month	$\sigma(\text{med})$	$\sigma(\text{ins})$	$\sigma(\text{med})$	$\sigma(\text{ins})$
May17	0.23	0.31	7.80	10.64
June17	0.28	0.32	9.72	11.04
July17	0.26	0.33	8.93	11.34
Aug.17	0.27	0.39	9.02	13.24
Sept.17	0.13	0.26	4.19	8.41
Oct.17	0.08	0.20	2.63	6.10
No.17	0.11	0.19	3.53	5.75
Dec.17	0.16	0.25	4.80	7.45
Jan.18	0.22	0.33	6.45	9.38
mean	0.19	0.29	6.34	9.26
	MUF			
GRK	MHz	MHz	%	%
month	$\sigma(\text{med})$	$\sigma(\text{ins})$	$\sigma(\text{med})$	$\sigma(\text{ins})$
May17	2.05	2.81	17.50	23.74
June17	1.82	2.42	14.51	19.25
July17	1.62	2.53	13.31	20.97
Aug.17	1.83	2.78	16.09	24.24
Sept.17	1.43	2.59	12.90	22.13
Oct.17	1.43	2.92	12.58	23.50
No.17	1.90	2.86	20.40	24.88
Dec.17	1.42	2.44	16.84	24.62
Jan.18	2.45	3.53	28.27	32.19
mean	1.77	2.76	16.93	23.95

Estimates for instantaneous values refer to cases when model (median) values are used as daily magnitudes. In this case, deviations should increase because of variations day by day. Absolute errors are given in units of

measurement, relative errors in %. The last line gives the average values.

Table 2. The standard deviations of the model parameters M3000F2 and MUF3000F2 from the experimental values for the Lovozero station

	M3000			
LOZ			%	%
month	$\sigma(\text{med})$	$\sigma(\text{ins})$	$\sigma(\text{med})$	$\sigma(\text{ins})$
May17	0.11	0.16	3.42	5.15
June17	0.15	0.17	4.85	5.52
July17	0.16	0.20	5.21	6.48
Aug.17	0.28	0.38	8.79	11.66
Sept.17	0.12	0.16	3.86	4.84
Oct.17	0.18	0.36	5.49	10.66
Nov.17	0.17	0.21	5.03	6.13
Dec.17	0.26	0.28	8.06	7.97
Jan.18	0.22	0.33	6.45	9.38
mean	0.18	0.25	5.68	7.53
	MUF			
LOZ	MHz	MHz	%	%
month	$\sigma(\text{med})$	$\sigma(\text{ins})$	$\sigma(\text{med})$	$\sigma(\text{ins})$
May17	1.24	1.48	9.81	11.65
June17	0.95	1.61	7.46	11.90
July17	1.50	1.98	11.63	15.11
Aug.17	1.86	2.55	15.16	20.18
Sept.17	2.19	2.56	18.87	20.46
Oct.17	2.06	3.77	17.79	28.62
Nov.17	2.69	3.23	27.26	27.40
Dec.17	3.04	2.82	35.40	27.14
Jan.18	2.45	3.53	28.27	32.19
mean	2.0	2.61	19.07	21.63

A microscopic difference is seen between the average error values for the two stations. Seasonal dependence is identical also. There is a big difference between day and night values in the winter. In the summer, variations are small because of sun position. Table 3 shows the average annual errors in determining the parameters M3000F2 and MUF3000F2 along with estimates for the standard parameters foF2 and hmF2.

The average estimates of Table 3 are significantly less than the estimates [4] for the polar cap and are close to the mid-latitude values.

It is interesting to notice, that there is no essential difference of values in Table 3 for both stations, despite a difference of latitudes.

Table 3. Average values of σ , %, characterizing the correspondence between the model and the experiment

mean	GRK		LOZ	
	med	ins	med	ins
foF2	10.80	14.61	12.46	14.10
hmF2	22.32	26.17	22.05	26.15
M3000F2	6.34	9.26	5.68	7.53
MUF3000F2	16.93	23.95	19.07	21.63

2.2 Comparison of Values Calculated by the Ray Tracing Method on the GRK-LOZ Path

A comparison was made for a month characterized by the lowest level of solar activity, as can be seen from Figure 2 for monthly averages of the index F10.7.

The calculations were carried out using the method of characteristics using the original IRI model and its adaptation to the parameters of the current diagnostics. The results are shown in Figure 3 for 33 cases. The red dots indicate the experimental values, the black squares refer to the results for the original IRI model, the green triangles represent the curve for the IRI model adapted to the foF2 values measured at the ends of the path, since they are most often available. Diamonds represent a curve for the IRI model adapted to foF2 and hmF2 values. It can be seen that each next step increases compliance. The SMSE for these options was 31.4%, 25%, and 17.2%.

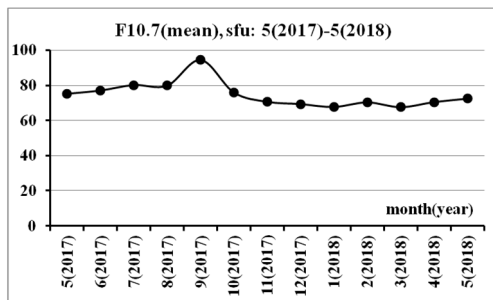


Figure 2. The level of solar activity in the period, including the considered years

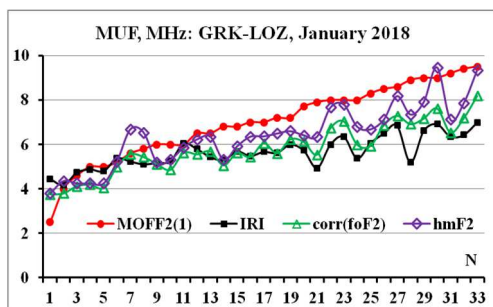


Figure 3. Comparison of the MUF for various options using the ray tracing method on the Gorkovskaya - Lovozero path in January 2018

2.3 Comparison of MUF Values Calculated Using the MD Coefficient

There is a simple and fairly reliable way to determine the MUF according to the characteristics in the middle of the path: $MUF(D) = MD * foF2(D/2)$. This is especially true for fairly short paths. As can be seen from subsection 2.1, there are experimental and model values of M3000F2. They can be counted for the length D of any path [5]. In this case D is ~ 900 km. In the given paper, we tested several options that are possible in a real situation. Firstly, the absence of any a priori experimental data. In this case, $MUF(D) = MD(IRI)*foF2(IRI)$. Secondly, values of the critical frequencies foF2 may be available at the ends of the path. Then the easiest way is to determine the half-sum of these values. The third option involves the use of the total electron content TEC of the ionosphere. In this case, there were values of foF2 at the ends of the path. To calculate the TEC, we used the GIM-JPL map from IONEX files on the website <ftp://cdis.gsfc.nasa.gov/pub/gps/products/ionex/>. Since it is necessary to know the equivalent slab thickness τ of the ionosphere to determine foF2 using TEC, it was calculated from the experimental data of foF2 and TEC at the ends of the path. Then the experimental values of TEC(D/2) and a half-sum of equivalent slab thicknesses were used to calculate foF2(D/2). The obtained values are shown in Figure 4.

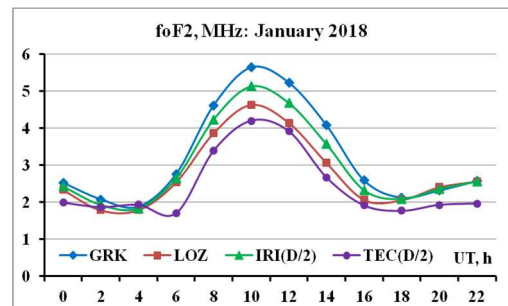


Figure 4. The values of the critical frequencies foF2 in the middle of the path to determine the MUF

To determine the MUF, these values were multiplied by the MD coefficient. The results are shown in Figure 5.

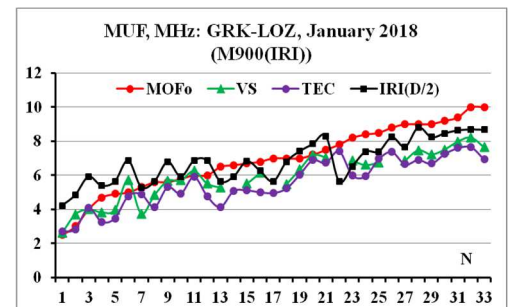


Figure 5. Comparison of the MUF for various options by the Smith method on the path Gorkovskaya - Lovozero in January 2018

The average absolute deviations were 0.92 MHz for the original IRI model, 1.03 MHz for the use of vertical sounding data at the ends of the path, and 1.36 MHz for using TEC.

The standard deviation for these cases was 1.09 MHz, 1.23 MHz and 1.6 MHz. Relative errors are 15.77%, 17.85% and 23.13%. It can be seen that in this case, a simple method using the original IRI model gave a result comparable to the ray tracing method with adjusting the model to a complete set of VS data. The overpriced error of the method using TEC, which proved to be good in conditions of high solar activity [6], is associated with a large difference in τ at the ends of the path, as can be seen from Figure 6.

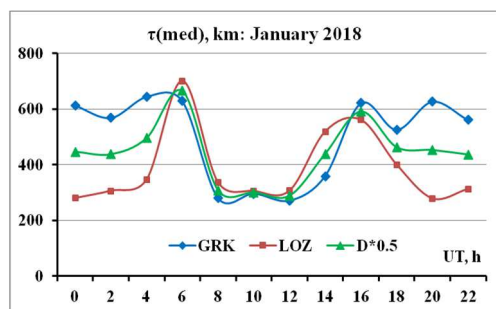


Figure 6. Obtained medians of equivalent slab thickness $\tau(\text{med})$ in the middle of the path

It is possible that in this case the best result will be given by the method [7].

3 Conclusion

Areas of high latitudes are insufficiently equipped with measuring instruments. In addition, there are known difficulties in sounding the high-latitude ionosphere due to its great variability under the influence of geophysical factors. Therefore, even small data sets are of interest. In this paper, we used data from vertical and oblique sounding between two points Gorkovskaya and Lovozero. The same results have been obtained for other pairs of stations. Parameter differences between points and the IRI model are estimated. The main attention is paid to the assessment of the most important parameter - the maximum useable frequency MUF. It was found that the IRI model can be used not only in the adaptation option to the parameters of the current diagnostics in the ray tracing method, but also in determining the propagation coefficient and critical frequency in the middle of the short path. The results relate to conditions of low solar activity. An amazing result was obtained using the total electron content of the ionosphere to determine the values of the critical frequency and requires additional confirmation. This is all the more important because the activity of the Sun is falling and will remain low in the coming years. This is confirmed by forecasts of solar activity, for example, in the paper [8] and the graph on the website <https://www.swpc.noaa.gov/products/predicted-sunspot-number-and-radio-flux>.

4 Acknowledgements

Authors express the gratitude to employees of the Arctic and Antarctic scientific research institute for providing data of vertical and oblique sounding on a site <http://geophys.aari.ru/>, Community Coordinated Modeling Center for granting of model IRI online. Authors thank organizations and scientists providing data of JPL maps. The results were obtained in the framework of the state task of the Ministry of Science and Higher Education of Russia (State assignment in the field of scientific activity, Southern Federal University, № 0852-2020-0015).

7 References

1. H. Lühr, and C. Xiong, "IRI-2007 model overestimates electron density during the 23/24 solar minimum," *Geophys. Res. Lett.*, 2010, **37**, L23101, doi: 10.1029/2010GL045430.
2. D. Bilitza, D. Altadill, D. Truhlik, V. Shubin, I. Galkin, B. Reinisch, and X. Huang, "International Reference Ionosphere 2016: From ionospheric climate to real-time weather predictions", *Space Weather*, **15**, 2017, pp.418–429, doi: 10.1002/2016SW001593.
3. T. L. Gulyaeva, "Modification of solar activity indices in the international reference ionosphere IRI and IRI-PLAS models due to recent revision of sunspot number time series," *Solar-Terrestrial Physics*, **2**, March 2016, pp. 87-98, doi: 10.12737/20872.
4. D. R. Themens, P. T. Jayachandran, M. J. Nicolls, and J. W. MacDougall, "A top to bottom evaluation of IRI 2007 within the polar cap," *J. Geophys. Res. Space Physics*, **119**, August 2014, pp. 6689 – 6703, doi: 10.1002/2014JA020052.
5. G. V. Kotovich, A. G. Kim, S. Ya. Mikhailov, V. P. Grozov, and Ya. S. Mikhailov, "Determining the foF2 critical frequency at the path midpoint from oblique sounding data based on the Smith method," *Geomagnetism and Aeronomy*, **46**, 2006, pp. 547-551, doi: <https://doi.org/10.1134/S0016793206040141>.
6. D. V. Blagoveshchensky, O. A. Maltseva, M. M. Anishin, D. D. Rogov, and M. A. Sergeeva, "Modeling of HF propagation at high latitudes on the basis of IRI," *Adv. Space Res.*, May 2016, pp. 821–834, doi: <http://dx.doi.org/10.1016/j.asr.2016.05.027>.
7. D. D. Wijaya, H. Haralambous, C. Oikonomou, and W. Kuntjoro, "Determination of the ionospheric foF2 using a stand-alone GPS receiver," *J Geod.*, **91**, March 2017, pp. 1117–1133, doi: 10.1007/s00190-017-1013-21.
8. J. Javaraiah, "Will Solar Cycles 25 and 26 Be Weaker than Cycle 24?," *Solar Physics*, **292**, 2017, pp.1-13, doi: 10.1007/s11207-017-1197-x.